

Article

Enhanced Supercapacitor Performance by Harnessing Carbon Nanoparticles and Colloidal SnO₂ Quantum Dots

Tejaswi Tanaji Salunkhe ^{1,†}, Babu Bathula ^{2,†}, Il Tae Kim ¹, Vedyappan Thirumal ^{2,*} and Kisoo Yoo ^{2,*}

¹ Department of Chemical and Biological Engineering, Gachon University, Seongnam-si 13120, Republic of Korea; 201850068@gachon.ac.kr (T.T.S.); itkim@gachon.ac.kr (I.T.K.)

² School of Mechanical Engineering, Yeungnam University, Gyeongsan 38541, Republic of Korea; babuphysicist@ynu.ac.kr

* Correspondence: vedyappanthirumal@yu.ac.kr (V.T.); kisooyoo@yu.ac.kr (K.Y.)

† These authors contributed equally to this work.

Abstract: The creation of effective supercapacitor materials is still a priority in the quest to improve energy storage technology. Herein, we present a novel nanocomposite composed of carbon nanoparticles (CNPs) and colloidal SnO₂ quantum dots (c-SQDs) or colloidal SnO₂ ultrasmall nanoparticles, synthesized through a facile sonochemical-assisted hydrothermal approach. The XRD and XPS analyses confirmed the successful synthesis and composition of the CNP/c-SQD nanocomposite. Morphology studies revealed a well-dispersed morphology with intimate interfacial interactions between the CNPs and c-SQDs. Specifically, the nanocomposite exhibited a high specific capacitance of 569 F/g at a current density of 1 A/g, surpassing conventional carbon-based supercapacitors. Furthermore, the nanocomposite displayed excellent stability with 99% capacity retention after 5000 cycles, indicative of its superior cyclability. These results underscore the potential of the CNP/c-SQD nanocomposite as a promising electrode material for high-performance supercapacitor applications, offering enhanced charge storage capacity, stability, and cyclability. This study contributes to the advancement of energy storage technologies, paving the way for the development of efficient and sustainable electrochemical energy storage devices.

Keywords: supercapacitor; carbon nanoparticles; SnO₂ quantum dots; nanocomposite; electrochemical performance



Citation: Salunkhe, T.T.; Bathula, B.; Kim, I.T.; Thirumal, V.; Yoo, K.

Enhanced Supercapacitor Performance by Harnessing Carbon Nanoparticles and Colloidal SnO₂ Quantum Dots. *Crystals* **2024**, *14*, 482. <https://doi.org/10.3390/cryst14060482>

Academic Editor: Faxing Wang

Received: 22 April 2024

Revised: 17 May 2024

Accepted: 20 May 2024

Published: 21 May 2024



Copyright: © 2024 by the authors. Licensee MDPI, Basel, Switzerland. This article is an open access article distributed under the terms and conditions of the Creative Commons Attribution (CC BY) license (<https://creativecommons.org/licenses/by/4.0/>).

1. Introduction

The rapid expansion of renewable energy sources, the electrification of transportation, and the growing need for grid stabilisation have all contributed to an increase in the need for effective energy storage systems in recent years [1]. Supercapacitors, often referred to as electrochemical capacitors, have shown great promise in resolving these energy storage issues because of their long cycle life, high power density, and quick charge–discharge rates [2]. Supercapacitors store energy electrostatically, as opposed to normal batteries, which store energy through chemical reactions. This enables quick energy storage and release [3]. CNPs have garnered significant attention in the field of supercapacitors due to their unique properties, including high surface area, excellent electrical conductivity, and chemical stability [4]. These attributes make CNPs ideal candidates for electrode materials in supercapacitor devices, enabling efficient charge storage and high-power delivery [5]. Several studies have shown how CNPs can improve supercapacitors' performance, which results in better energy storage capacity, improved charge–discharge kinetics, and longer cycle life [6]. In addition to carbon-based materials, metal oxide nanomaterials have also emerged as promising candidates for supercapacitor applications [7]. Metal oxides, such as SnO₂, offer high theoretical capacitance, abundant redox-active sites, and favourable electrochemical properties, making them attractive for energy storage devices. The integration of metal oxide nanomaterials into supercapacitor electrodes has shown remarkable

improvements in capacitance, energy density, and stability, thus contributing to the advancement of supercapacitor technology [8,9]. Furthermore, the combination of carbon and metal oxide nanomaterials into nanocomposites has received considerable attention in recent years [10]. By combining the high surface area and conductivity of carbon materials with the pseudocapacitive behaviour and ion storage capacity of metal oxides, these hybrid materials take advantage of the complementary properties of both constituents [9]. Such nanocomposites offer enhanced electrochemical performance, including higher capacitance, improved rate capability, and superior cycling stability, positioning them as promising candidates for next-generation supercapacitor electrodes [11,12].

Among metal oxide nanomaterials, tin dioxide (SnO_2) has emerged as a highly attractive candidate for supercapacitor applications [13,14]. SnO_2 exhibits excellent electrochemical properties, including good chemical stability, and low cost, making it an ideal material for energy storage devices [15]. Moreover, the recent advancements in synthesizing SQDs have opened new avenues for enhancing supercapacitor performance [16–18]. Colloidal-SQDs possess unique quantum confinement effects, leading to improved charge storage kinetics and enhanced electrochemical activity compared to bulk materials. The synergistic combination of SQDs with different carbon-based materials, MoS_2 , and TiO_2 as nanocomposites holds great promise for further enhancing supercapacitor performance [19,20]. By carefully tailoring the composition and structure of these nanocomposites, researchers can achieve superior electrochemical properties, including higher capacitance, improved rate capability, and enhanced cycling stability. Thus, there exists a compelling need to explore the potential of SQDs in conjunction with other materials for advanced supercapacitor applications [21].

SnO_2 was synthesized on mesoporous carbon spheres with a hollow double-shell structure via the hydrothermal method for supercapacitor applications [22]. The composite exhibited characteristic redox peaks in the cyclic voltammetry (CV) curves, indicative of pseudocapacitive behaviour, with a specific capacitance of 470 F/g at a current density of 2 A/g and a cyclic stability of 88.4% after 4000 cycles. A SnO_2 @C composite was fabricated where a thin carbon layer encapsulated hollow tin oxide microspheres [23]. The primary limitation of this hollow-sphere structure was suboptimal electron transport, resulting in a specific capacitance of only 25.88 F/g at a current density of 0.1 A/g. Using ethanol thermal carbonization and steam activation, a SnO_2 @C composite with a mosaic structure was synthesized, where porous carbon microspheres served as hosts for SnO_2 nanoparticles [24]. This composite demonstrated a specific capacitance of 420 F/g at a current density of 1 A/g, with an energy density of 34.2 Wh/kg and a power density of 125 W/kg. After 2000 cycles, the specific capacitance retention was 91%. Carbon nanofibers (CNFs) were electrospun onto tin foil, and SnO_2 nanoparticles were then deposited via a solvothermal method [25]. The high surface area and well-exposed SnO_2 nanoparticles in this heterostructure facilitated rapid ion transport from the electrolyte to the SnO_2 surface, achieving a specific capacitance of 195 F/g at a scan rate of 0.3 A/g. The one-dimensional CNF structure enhanced conductivity, reduced charge transfer resistance, and maintained kinetic and thermodynamic stability, providing a cyclic stability of 95% after 1000 cycles.

In this context, the present work focuses on the synthesis and characterization of a novel nanocomposite comprising CNPs and c-SQDs for supercapacitor applications. By combining the advantages of both carbon and metal oxide nanomaterials, this nanocomposite aims to deliver superior electrochemical performance, addressing the growing demand for efficient and sustainable energy storage solutions. The subsequent sections of this paper will detail the preparation methods, characterization techniques, and electrochemical performance evaluation of the CNP/c-SQD nanocomposite, elucidating its potential for practical supercapacitor applications.

2. Materials and Methods

Conductive carbon nanoparticles were synthesized from glucose through a hydrothermal method following established protocol [26] and functionalized with nitric acid [27]. The

preparation of colloidal SnO₂ quantum dots proceeded as follows: initially, 0.3 g of thiourea (CH₄N₂S) and 0.9 g of tin chloride dihydrate (SnCl₂·2H₂O) were dispersed thoroughly in 30 mL of water. Subsequently, the resulting white solution was stirred at room temperature for 24 h, yielding a yellow solution containing colloidal SnO₂ quantum dots. The nanocomposite of carbon nanoparticle–colloidal SnO₂ quantum dots (CNP/c-SQD) was synthesized using a sonochemical approach. Specifically, 30 mg of carbon nanoparticles were dispersed in 40 mL of ethanol for 15 min. Then, 5 mL of c-SQDs were added dropwise to the CNP solution under stirring, followed by continued stirring for an additional 5 min. The mixture was subjected to probe sonication for 2 h and subsequently transferred to a 100 mL hydrothermal autoclave, which was placed in an oven at 150 degrees Celsius for 24 h (Figure 1).

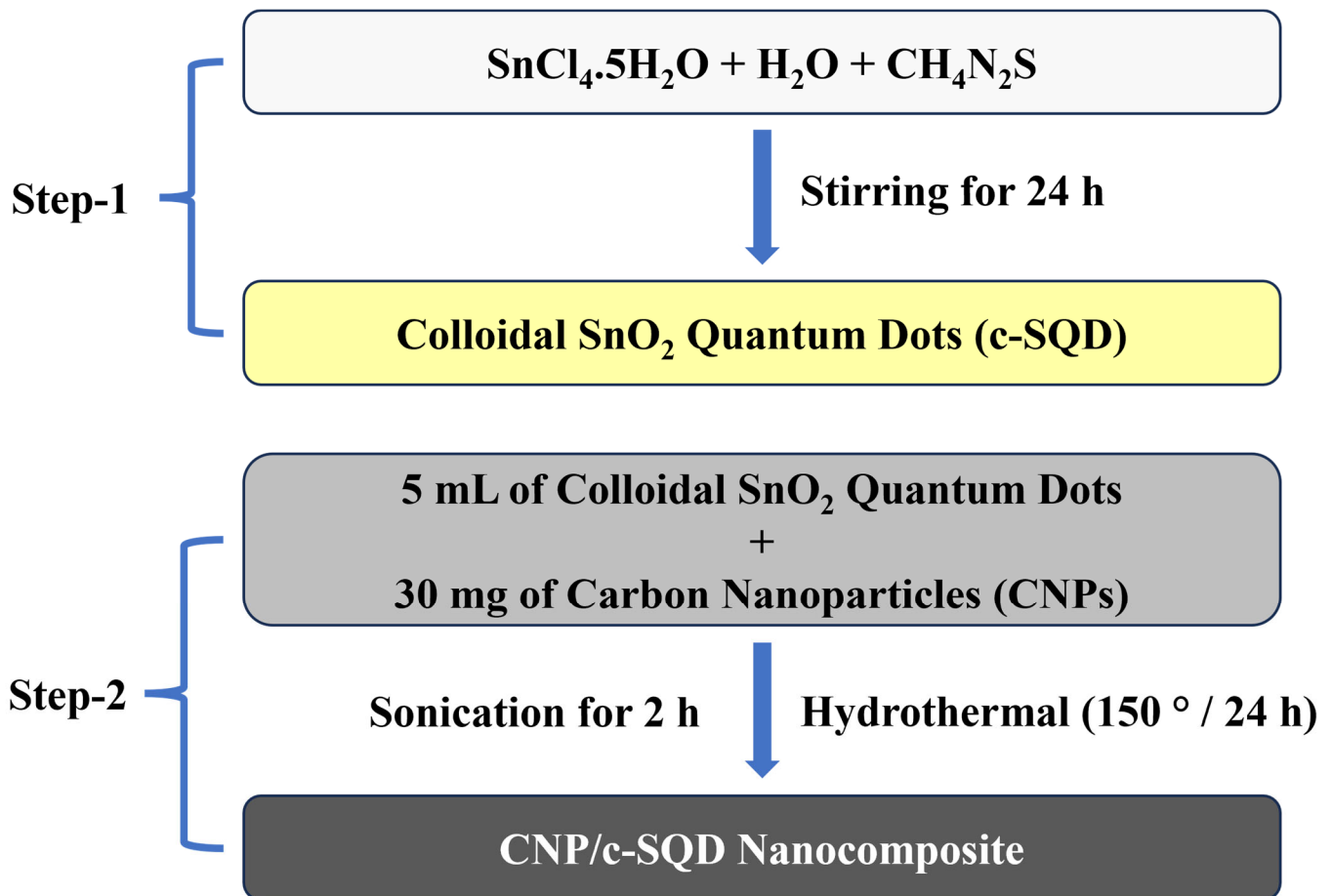


Figure 1. Flow-chart of the experimental procedure of the CNP/c-SQD nanocomposite.

Several analytical methods were employed to evaluate the synthesised nanostructures' morphological and structural properties. To determine the phase composition, X-ray diffraction (XRD) examination was performed using a PANalytical X'pert PRO apparatus (Amsterdam, The Netherlands). Scanning electron microscopy (SEM) imaging was performed with a Hitachi S-4800 instrument (Tokyo, Japan) to examine the surface morphology. Additionally, high-resolution transmission electron microscopy (HR-TEM) analysis was carried out using a G2 F30 S-Twin instrument from the USA to investigate the detailed nanostructure. Using equipment purchased from Thermo Fisher Scientific (Dreieich, UK), X-ray photoelectron spectroscopy (XPS) was used to analyse the elemental composition of the surface.

A composite mixture consisting of 80% CNP/c-SQD nanocomposite, 10% activated carbon (AC), and 10% polyvinylidene fluoride (PVDF) binder was formed to prepare the

electrode and coatings. To create a homogeneous composite that ensures excellent binding with PVDF and constant dispersion, the components were carefully mixed. This thoroughly blended composite was then applied to a substrate made of nickel foam (Ni-foam) to function as the current collector. Care was taken during the coating process to ensure that the Ni-foam was evenly covered, facilitating effective charge transfer, and improving electrode performance overall. The Ni-foam covered with the composite was annealed in an oven for an entire night at 80 °C to improve the adhesion and conductivity of the active material even more. This electrode arrangement, which capitalises on the inherent conductivity and distinctive features of the composite materials, offers a viable path for improved energy storage applications. It is characterised by the synergistic integration of CNP/c-SQD nanocomposite, AC, and PVDF.

3. Results

In the X-ray diffraction (XRD) analysis of the carbon nanoparticle/SnO₂ quantum dot nanocomposite (Figure 2a), the spectrum prominently features peaks at positions 26.72°, 34.28°, 51.87°, and 65.37°, corresponding to the tetragonal phase of SnO₂, as classified under the JCPDS card No: 01-0625 [28]. These peaks are ascribed to the (110), (101), (211), and (301) planes of the tetragonal SnO₂, which belongs to the space group P42/mnm with space group number 136. The predominance of these peaks suggests a significant presence of colloidal SnO₂ quantum dots, characterized by their ultra-small size which leads to broad XRD peaks. The absence of distinct peaks from the carbon nanoparticles (CNPs) in the nanocomposite can be attributed to several factors: the potential amorphous nature of the CNPs, which would not produce sharp XRD peaks; the possibility that the CNP content is too low, thus diluting their diffraction signals; or the overlap of their diffraction signals with the dominant SnO₂ peaks. This analysis indicates that the SnO₂ component of the nanocomposite is well characterized and dominant in the diffraction pattern [15].

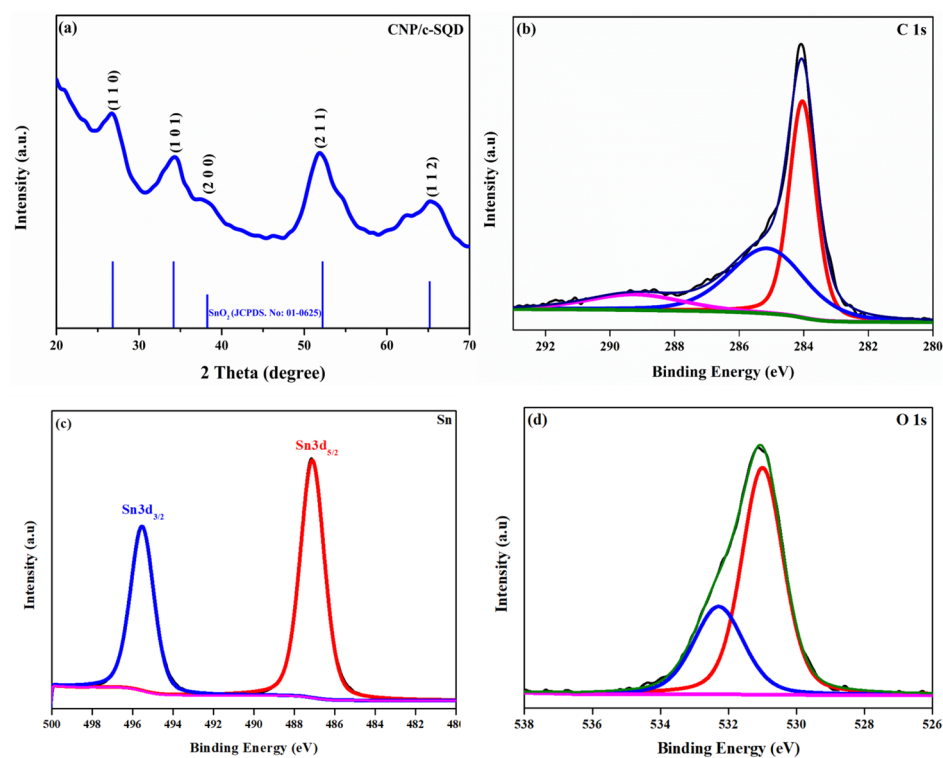


Figure 2. (a) XRD of the CNP/c-SQD nanocomposite and (b–d) high-level XPS spectra of C, Sn and O, respectively.

The X-ray photoelectron spectroscopy (XPS) analysis of Figure 2b–d elucidates the oxidation states and bonding environment of the elements within the carbon nanoparticle/SnO₂

quantum dot (CNP/c-SQD) nanocomposite. The comprehensive spectrum indicates the intricate details of the material's surface chemistry. Figure 2b illustrates the C 1s core-level spectra, exhibiting three peaks at binding energies of 284.05 eV, 285.17 eV, and 289.14 eV. The peak at 284.05 eV typically corresponds to the C-C bonding in sp^2 hybridized carbon, indicative of graphitic or amorphous carbon [29]. The peak at 285.17 eV is likely attributed to the C-O bonding, suggesting the presence of oxygen-containing functional groups, which may be integral to the composite's interface with SnO_2 . The peak at 289.14 eV may be due to more oxidised carbon species such as carboxylates or to $\pi-\pi^*$ shake-up satellites, which are a feature of aromatic carbon structures. Figure 2c presents the Sn 3d core-level spectra with two pronounced peaks at approximately 487.11 eV for $Sn3d_{5/2}$ and 495.53 eV for $Sn3d_{3/2}$, reflecting the spin-orbit splitting inherent to Sn atoms. The 8.42 eV separation between these peaks is characteristic of the Sn^{4+} oxidation state, corroborating the presence of SnO_2 as the primary oxide form in the quantum dots [30]. Figure 2d depicts the O 1s core-level spectra with two major peaks at around 531 eV and 532.29 eV, respectively. The higher binding energy peak around 532.29 eV is typically associated with oxygen vacancies or deficient regions, which are crucial for performance as they may act as active sites [31,32]. The peak at 531 eV suggests a binding environment of oxygen atoms coordinated with tin, further supporting the formation of SnO_2 . The data suggest that the CNP/c-SQD nanocomposite is well formed, with SnO_2 quantum dots displaying a tetragonal crystal structure and a stoichiometric oxidation state that is conducive to applications requiring specific valency and electronic structure, such as in photocatalysis or supercapacitor applications. The combination of carbon with SnO_2 in the nanocomposite may enhance electrical conductivity and provide a robust framework for electron transfer, vital for their performance in energy storage or catalysis. Typically, such figures from XPS analysis would complement the chemical state information with topographical and size distribution data, which are critical for correlating the surface chemistry with the physical structure of the nanocomposite.

Figure 3 provides a comprehensive series of images capturing the morphological nuances of pristine carbon nanoparticles (CNPs) and their nanocomposite with colloidal SnO_2 quantum dots (c-SQDs). The analysis of these images reveals key structural features significant for the nanocomposite's potential applications. Panel (a) of Figure 3 shows a scanning electron microscopy (SEM) image of pristine CNPs. The particles are characterized by an interconnected structure, which could be indicative of a high surface area conducive to enhanced interaction with c-SQDs. The smooth surface morphology seen in the pristine CNPs suggests a relatively defect-free structure that could facilitate uniform coverage by the c-SQDs. Panels (b) through (d) transition from SEM to transmission electron microscopy (TEM) images of the CNP/c-SQD nanocomposite, revealing a progression toward finer detail. In (b), the SEM image of the nanocomposite displays a core-shell-like structure, where the CNPs appear to serve as the core upon which the c-SQDs are anchored. This is due to the c-SQDs' extremely small size and colloidal nature, allowing them to fully attach and possibly envelop the CNPs [33]. This intimate connection suggests a strong interaction between the two components, which could enhance the nanocomposite's electrical and catalytic properties. The TEM images in (c) and (d) offer a more detailed examination, highlighting the ultra-small size of the c-SQDs and their pervasive distribution across the CNPs. The near-continuous coverage observed may lead to a synergistic effect, whereby the CNPs provide a conductive scaffold enhancing electron transfer, and the c-SQDs contribute to the active surface, possibly affecting the photocatalytic or electrochemical performance of the nanocomposite. This core-shell configuration could be particularly advantageous for applications requiring a high interface area between the conductive core and the active shell in energy storage systems [34]. Moreover, the morphological characteristics depicted, including the homogeneity and extent of the c-SQDs' attachment to the CNPs, are crucial for the functional performance of the nanocomposite. Overall, the morphology elucidated by Figure 3 paints a picture of a well-engineered nanocomposite material with a potential for high performance in its intended applications, thanks to the intricate architecture of CNPs and c-SQDs. The nanoscale organization, as visualized in these images, underscores

the advanced level of material synthesis and the potential for tailored functionalities in the CNP/c-SQD system.

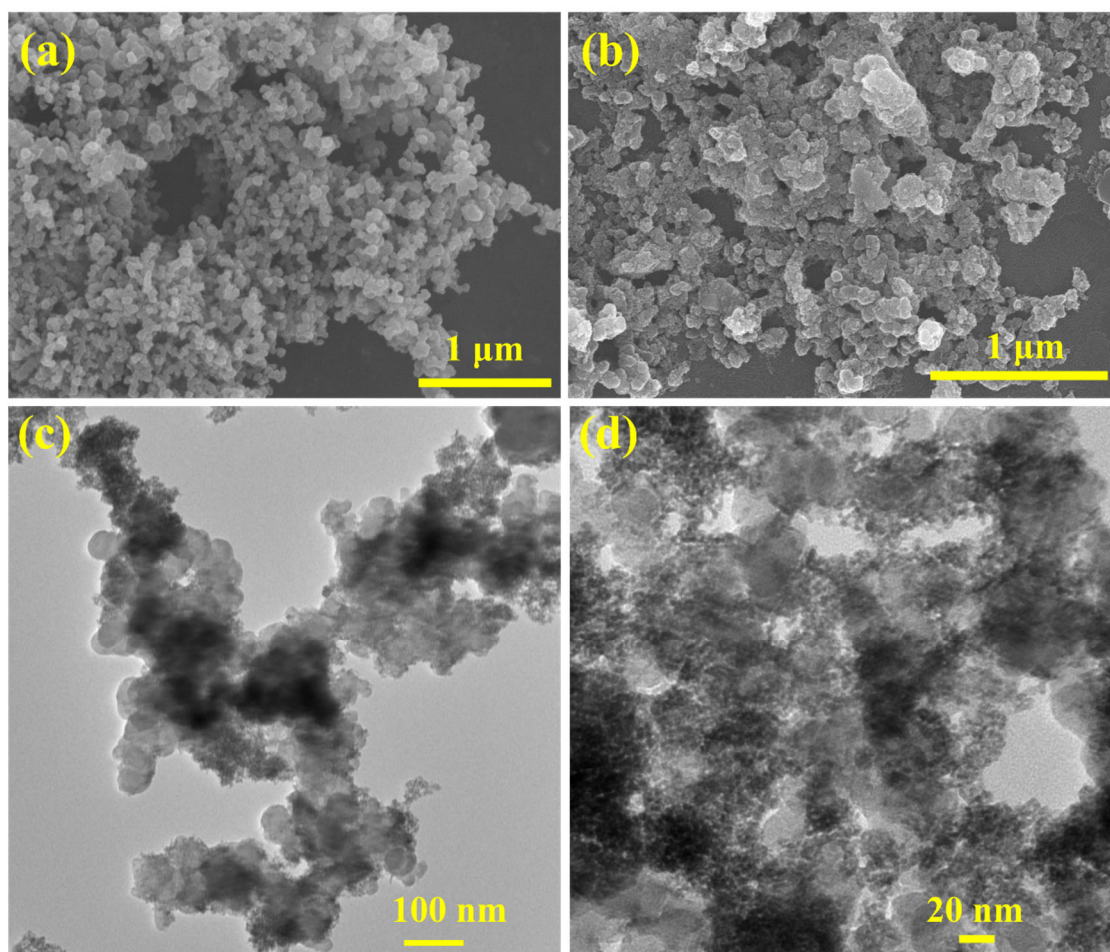


Figure 3. (a) SEM image of pristine CNPs, and (b–d) SEM and TEM images of the CNP/c-SQD nanocomposite.

Using a three-electrode arrangement submerged in a 3M KOH electrolyte, the electrochemical properties of CNPs and the CNP/c-SQD nanocomposite were thoroughly studied. In the Supplementary Material, the experimental setup and procedures are described in detail. A key component of the analysis was the use of cyclic voltammetry (CV), the results of which are shown in Figure 4a,b. Cyclic voltammograms were taken within a potential window of 0–0.6 V, at different scan rates from 10 to 100 mV/s. The overall area under the cyclic voltametric curves showed a discernible increase with high scan rates, suggesting the presence of the pseudocapacitive behaviour of the CNP-SQD nanocomposite [35]. The presence of these redox peaks can be attributed to oxygen-containing functional groups introduced during the acid treatment. Such functional groups, including carboxyl, hydroxyl, and others, can undergo reversible redox reactions, which contribute to the pseudocapacitance observed in the CV curves. This modification not only enhances the specific capacitance but also complements the inherent EDLC behaviour of the carbon material, leading to improved overall electrochemical performance. The CV profile of the CNP/c-SQD nanocomposite showed remarkably higher anodic and cathodic peak current than those of the CNPs. This finding is supported by the fact that the cyclic voltammograms forms did not change at any scan rate. Furthermore, an increase in both the anodic and cathodic peak currents correlated with an increase in scan rates, suggesting that the electrolyte's redox processes accelerated at higher scan rates. The electrons and ions were

able to flow more freely due to this acceleration, which improved their contact with the electrode surface. Interestingly, the main ions controlling these redox processes were found to be hydroxide ions. Notably, adsorption was a part of the oxidation process, whereas hydroxide ions were released during the reduction step. The quick movement of charges at these high scan rates also led to the observation of peak shifts, which were explained by the system's inability to properly react in time. Even so, the general form of the CV curves was very constant throughout the scan rate range, highlighting the remarkable rate capabilities and capacitive effects of the CNP/c-SQD nanocomposite. Despite this, the basic forms of the CV curves did not change, demonstrating the exceptional electrochemical stability and rate capacity of the CNP/c-SQD nanocomposite.

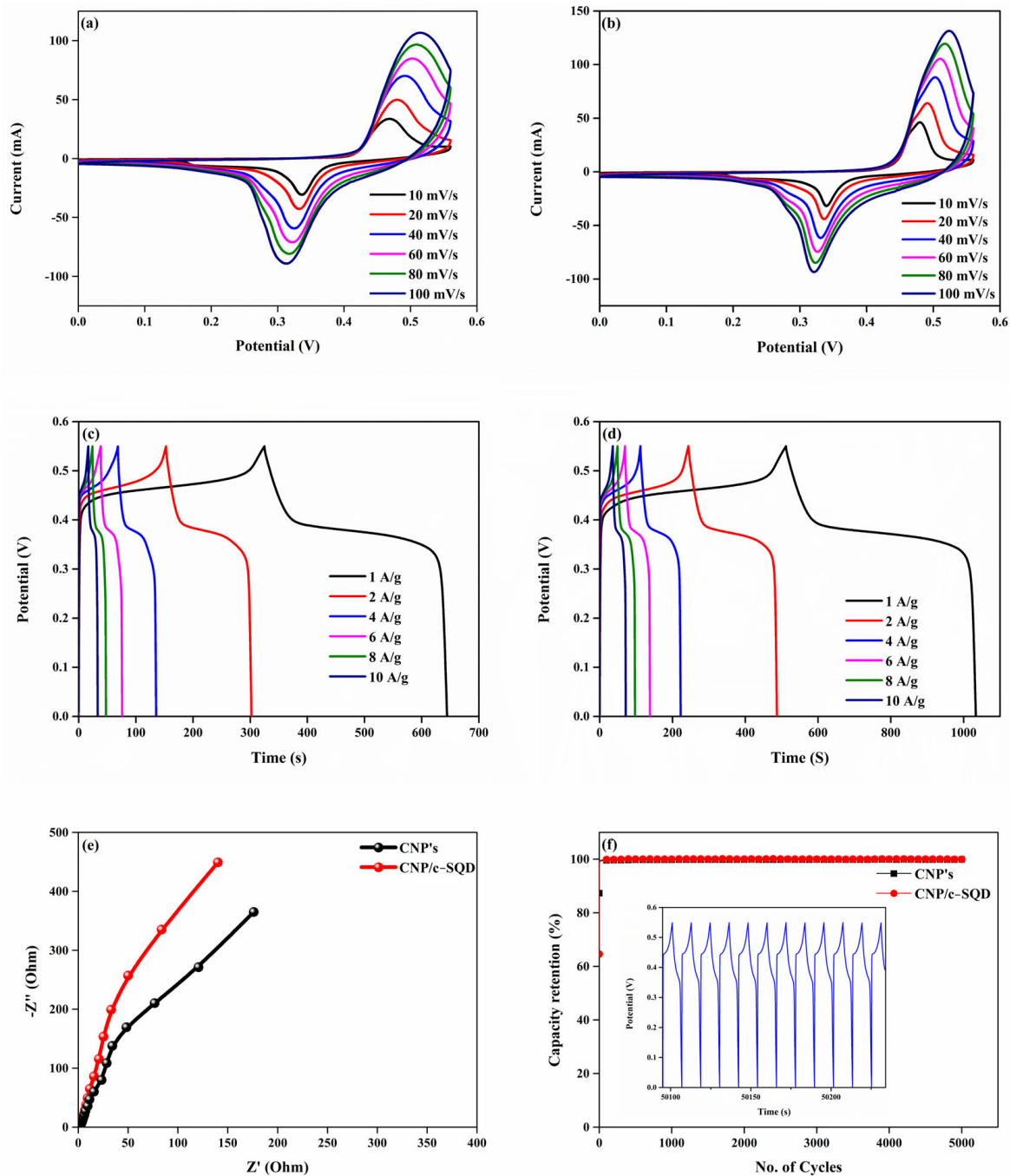


Figure 4. CV plot of CNPs (a) and CNP/c-SQD (b); GCD profiles of CNPs (c) and CNP/c-SQD (d); EIS (e) and capacity retention vs. number of cycles (f) of CNPs and the CNP/c-SQD nanocomposite.

The galvanostatic charge–discharge (GCD) curves for all prepared samples, including CNPs and the CNP/c-SQD nanocomposite, are depicted in Figure 4b,c, providing insights into their charge–discharge behaviour under constant current density conditions (1 to 10 A/g). The charge–discharge process was conducted within the potential range of 0–0.55 V across various current densities for each sample. The specific capacitance values of CNPs and the CNP/c-SQD nanocomposite at a current density of 1 A/g were determined to be 358 F/g and 569 F/g, respectively. This increase in specific capacitance observed in the CNP/c-SQD nanocomposite compared to pristine CNPs can be attributed to the robust interaction between the CNPs and c-SQDs. Furthermore, the effect of increasing current density on the charge–discharge behaviour was investigated by incrementally raising the applied current from 1 to 10 A/g. As expected, with the escalation in current density, a decrease in specific capacitance was observed due to deteriorating electrochemical kinetics at higher current densities. The plateau evident in the charge–discharge plots underscores the pronounced pseudocapacitive behaviour exhibited by the materials. To assess the internal resistance of carbon nanoparticles and the CNP/c-SQD nanocomposite, electrochemical impedance spectroscopy (EIS) measurements were conducted. The Nyquist plots depicted in Figure 4e reveal low internal resistance for both CNPs and the CNP/c-SQD nanocomposite. Notably, the CNP/c-SQD nanocomposite exhibited notably lower charge transfer resistance compared to CNPs alone [36]. This can be attributed to the nanocomposite's provision of additional active sites for charge storage and the facilitation of faster ion transport. Consequently, the CNP/c-SQD nanocomposite demonstrated a higher specific capacitance of 570 F/g, resulting in enhanced charge–discharge cycling performance. Furthermore, as shown in Figure 4f, the cycle stability of CNPs and the CNP-SQD nanocomposite was assessed using the same electrolyte parameters, keeping a steady current of 10 A/g across 5000 charge–discharge cycles within the potential window of 0–0.55 V. The cycle stabilities of CNPs and the CNP/c-SQD nanocomposite were found to be remarkably strong, with values of roughly greater than 99%, indicating their potential for long-term energy storage applications.

4. Conclusions

In conclusion, this study comprehensively explored the synthesis, characterization, and electrochemical performance of a CNP/c-SQD nanocomposite for supercapacitor application. The nanocomposite exhibited superior electrochemical properties, including enhanced specific capacitance, excellent rate capability, and remarkable cycling stability. The nanocomposite's favourable charge storage kinetics and pseudocapacitive behaviour were discovered through electrochemical investigations that included cyclic voltammetry and galvanostatic charge–discharge experiments. Low internal resistance was also shown by means of electrochemical impedance spectroscopy, which suggests effective charge transport within the nanocomposite. These results demonstrate the potential of CNP/c-SQD nanocomposites as viable electrode materials for cutting-edge energy storage devices, making major contributions to the creation of high-performing and environmentally friendly supercapacitors.

Supplementary Materials: The following supporting information can be downloaded at: <https://www.mdpi.com/article/10.3390/cryst14060482/s1>, Figure S1: XPS survey spectrum of CNP/c-SQD nanocomposite; Figure S2: Transmission electron microscope (TEM) image of SnO₂-QDs, Figure S3: CV curve for the bare nickel foam and CNPs at a scan rate of 100 mV/s.

Author Contributions: Conceptualization, methodology, validation, and writing—original draft preparation, T.T.S.; formal analysis, resources, data curation, and writing—original draft preparation, B.B.; writing—review and editing, and supervision, I.T.K.; formal analysis, resources, data curation, and writing—original draft preparation, V.T.; writing—review and editing, and supervision, K.Y. All authors have read and agreed to the published version of the manuscript.

Funding: This work was funded by the Ministry of Trade, Industry and Energy (MOTIE, Korea) under the Materials and Parts Technology Development Programme (20019447, Development of PI(Polyimide) separator manufacturing technology and equipment for 300 °C high heat-resistance lithium secondary battery).

Data Availability Statement: The original contributions presented in the study are included in the article/Supplementary Material; further inquiries can be directed to the corresponding author/s.

Conflicts of Interest: The authors declare that they have no conflict of interest regarding the publication of this article, financial and/or otherwise.

References

1. Hossain, E.; Faruque, H.M.R.; Sunny, M.S.H.; Mohammad, N.; Nawar, N. A Comprehensive Review on Energy Storage Systems: Types, Comparison, Current Scenario, Applications, Barriers, and Potential Solutions, Policies, and Future Prospects. *Energies* **2020**, *13*, 3651. [CrossRef]
2. Yadlapalli, R.T.; Alla, R.R.; Kandipati, R.; Kotapati, A. Super capacitors for energy storage: Progress, applications and challenges. *J. Energy Storage* **2022**, *49*, 104194. [CrossRef]
3. Kumar, N.; Kim, S.-B.; Lee, S.-Y.; Park, S.-J. Recent Advanced Supercapacitor: A Review of Storage Mechanisms, Electrode Materials, Modification, and Perspectives. *Nanomaterials* **2022**, *12*, 3708. [CrossRef] [PubMed]
4. Tatrari, G.; Karakoti, M.; Tewari, C.; Pandey, S.; Bohra, B.S.; Dandapat, A.; Sahoo, N.G. Solid waste-derived carbon nanomaterials for supercapacitor applications: A recent overview. *Mater. Adv.* **2021**, *2*, 1454–1484. [CrossRef]
5. Yadav, S.; Daniel, S. Green synthesis of zero-dimensional carbon nanostructures in energy storage applications—A review. *Energy Storage* **2024**, *6*, e500. [CrossRef]
6. Li, Y.; Zhao, F.-G.; Liu, L.-N.; Xu, Z.-W.; Xie, G.; Li, J.; Gao, T.; Li, W.; Li, W.-S. Carbon Nanomaterials-Enabled High-Performance Supercapacitors: A Review. *Adv. Energy Sustain. Res.* **2023**, *4*, 2200152. [CrossRef]
7. Xu, Q.; Niu, Y.; Li, J.; Yang, Z.; Gao, J.; Ding, L.; Ni, H.; Zhu, P.; Liu, Y.; Tang, Y.; et al. Recent progress of quantum dots for energy storage applications. *Carbon Neutrality* **2022**, *1*, 13. [CrossRef]
8. Liao, S.-Y.; Chen, J.; Cui, S.-F.; Shang, J.-Q.; Li, Y.-Z.; Cheng, W.-X.; Liu, Y.-D.; Cui, T.-T.; Shu, X.-G.; Min, Y.-G. CoS₂ enhanced SnO₂@rGO heterostructure quantum dots for advanced lithium-ion battery anode. *J. Power Sources* **2023**, *553*, 232265. [CrossRef]
9. Yadav, M.S. Metal oxides nanostructure-based electrode materials for supercapacitor application. *J. Nanoparticle Res.* **2020**, *22*, 367. [CrossRef]
10. Abou-Elyazed, A.S.; Hassan, S.; Ashry, A.G.; Hegazy, M. Facile, Efficient, and Cheap Electrode based on SnO₂/Activated Carbon Waste for Supercapacitor and Capacitive Deionization Applications. *ACS Omega* **2022**, *7*, 19714–19720. [CrossRef]
11. Wang, B.; Guan, D.; Gao, Z.; Wang, J.; Li, Z.; Yang, W.; Liu, L. Preparation of graphene nanosheets/SnO₂ composites by pre-reduction followed by in-situ reduction and their electrochemical performances. *Mater. Chem. Phys.* **2013**, *141*, 1–8. [CrossRef]
12. Kumar, R.; Nekouei, R.K.; Sahajwalla, V. In-situ carbon-coated tin oxide (ISCC-SnO₂) for micro-supercapacitor applications. *Carbon Lett.* **2020**, *30*, 699–707. [CrossRef]
13. Selvan, R.K.; Perelshtein, I.; Perkas, N.; Gedanken, A. Synthesis of Hexagonal-Shaped SnO₂ Nanocrystals and SnO₂@C Nanocomposites for Electrochemical Redox Supercapacitors. *J. Phys. Chem. C* **2008**, *112*, 1825–1830. [CrossRef]
14. Yang, Y.; Ren, S.; Song, X.; Guo, Y.; Si, D.; Jing, H.; Ma, S.; Hao, C.; Ji, M. Sn@SnO₂ attached on carbon spheres as additive-free electrode for high-performance pseudocapacitor. *Electrochim. Acta* **2016**, *209*, 350–359. [CrossRef]
15. Kedara Shivasharma, T.; Sahu, R.; Rath, M.C.; Keny, S.J.; Sankapal, B.R. Exploring tin oxide based materials: A critical review on synthesis, characterizations and supercapacitive energy storage. *Chem. Eng. J.* **2023**, *477*, 147191. [CrossRef]
16. Wang, L.; He, Y.; Liu, D.; Liu, L.; Chen, H.; Hu, Q.; Liu, X.; Zhou, A. SnO₂ Quantum Dots Interspersed d-Ti₃C₂T_x MXene Heterostructure with Enhanced Performance for Lithium Ion Battery. *J. Electrochem. Soc.* **2020**, *167*, 116522. [CrossRef]
17. Neelakanta Reddy, I.; Akkinapally, B.; Siva Kumar, N.; Asif, M.; Shim, J.; Bai, C. SnO₂ nanoparticles anchored on carbon spheres for enhanced charge generation and potentiodynamic effects. *J. Electroanal. Chem.* **2023**, *937*, 117411. [CrossRef]
18. Geng, J.; Ma, C.; Zhang, D.; Ning, X. Facile and fast synthesis of SnO₂ quantum dots for high performance solid-state asymmetric supercapacitor. *J. Alloys Compd.* **2020**, *825*, 153850. [CrossRef]
19. Vargheese, S.; Kumar, R.S.; Kumar, R.T.R.; Shim, J.J.; Haldorai, Y. Binary metal oxide (MnO₂/SnO₂) nanostructures supported triazine framework-derived nitrogen-doped carbon composite for symmetric supercapacitor. *J. Energy Storage* **2023**, *68*, 9. [CrossRef]
20. Veeresh, S.; Ganesha, H.; Nagaraju, Y.S.; Vijeth, H.; Devendrappa, H. Activated carbon incorporated graphene oxide with SnO₂ and TiO₂-Zn nanocomposite for supercapacitor application. *J. Alloys Compd.* **2023**, *952*, 11. [CrossRef]
21. Babu, B.; Babu Eadi, S.; Yoo, J.; Lee, H.-D.; Yoo, K. Core@shell nanorods for enhancing supercapacitor performance: ZnWO₄ nanorods decorated with colloidal SnO₂ quantum dots. *Mater. Lett.* **2023**, *343*, 134389. [CrossRef]
22. Yang, G.; Zhang, Z.; Zhang, Z.; Zhang, L.; Xue, Y.; Yang, J.; Peng, C. Rational construction of well-defined hollow double shell SnO₂/mesoporous carbon spheres heterostructure for supercapacitors. *J. Alloys Compd.* **2021**, *873*, 159810. [CrossRef]
23. Ren, S.; Yang, Y.; Xu, M.; Cai, H.; Hao, C.; Wang, X. Hollow SnO₂ microspheres and their carbon-coated composites for supercapacitors. *Colloids Surf. A Physicochem. Eng. Asp.* **2014**, *444*, 26–32. [CrossRef]

24. He, C.; Xiao, Y.; Dong, H.; Liu, Y.; Zheng, M.; Xiao, K.; Liu, X.; Zhang, H.; Lei, B. Mosaic-Structured SnO₂@C Porous Microspheres for High-Performance Supercapacitor Electrode Materials. *Electrochim. Acta* **2014**, *142*, 157–166. [[CrossRef](#)]
25. Mu, J.; Chen, B.; Guo, Z.; Zhang, M.; Zhang, Z.; Shao, C.; Liu, Y. Tin oxide (SnO₂) nanoparticles/electrospun carbon nanofibers (CNFs) heterostructures: Controlled fabrication and high capacitive behavior. *J. Colloid Interface Sci.* **2011**, *356*, 706–712. [[CrossRef](#)] [[PubMed](#)]
26. Tovar-Martinez, E.; Sanchez-Rodriguez, C.E.; Sanchez-Vasquez, J.D.; Reyes-Reyes, M.; López-Sandoval, R. Synthesis of carbon spheres from glucose using the hydrothermal carbonization method for the fabrication of EDLCs. *Diam. Relat. Mater.* **2023**, *136*, 110010. [[CrossRef](#)]
27. Phattharasupakun, N.; Wutthiprom, J.; Suktha, P.; Iamprasertkun, P.; Chanlek, N.; Shepherd, C.; Hadzifejzovic, E.; Moloney, M.; Foord, J.S.; Sawangphruk, M. High-performance supercapacitors of carboxylate-modified hollow carbon nanospheres coated on flexible carbon fibre paper: Effects of oxygen-containing group contents, electrolytes and operating temperature. *Electrochim. Acta* **2017**, *238*, 64–73. [[CrossRef](#)]
28. Zhang, M.; Ma, J.; Zhang, Y.; Lu, L.; Chai, Y.; Yuan, R.; Yang, X. Ion exchange for synthesis of porous Cu_xO/SnO₂/ZnSnO₃ microboxes as a high-performance lithium-ion battery anode. *New J. Chem.* **2018**, *42*, 12008–12012. [[CrossRef](#)]
29. Wu, Y.; Lin, Y.; Xu, J. Synthesis of Ag–Ho, Ag–Sm, Ag–Zn, Ag–Cu, Ag–Cs, Ag–Zr, Ag–Er, Ag–Y and Ag–Co metal organic nanoparticles for UV-Vis-NIR wide-range bio-tissue imaging. *Photochem. Photobiol. Sci.* **2019**, *18*, 1081–1091. [[CrossRef](#)]
30. Cao, Y.; He, T.; Zhao, L.; Wang, E.; Yang, W.; Cao, Y. Structure and phase transition behavior of Sn⁴⁺-doped TiO₂ nanoparticles. *J. Phys. Chem. C* **2009**, *113*, 18121–18124. [[CrossRef](#)]
31. Sahu, B.K.; Das, A. Significance of oxygen defects in SnO₂ quantum dots as hybrid electrochemical capacitors. *J. Phys. Chem. Solids* **2019**, *129*, 293–297. [[CrossRef](#)]
32. Asaithambi, S.; Sakthivel, P.; Karuppaiah, M.; Sankar, G.U.; Balamurugan, K.; Yuvakkumar, R.; Thambidurai, M.; Ravi, G. Investigation of electrochemical properties of various transition metals doped SnO₂ spherical nanostructures for supercapacitor applications. *J. Energy Storage* **2020**, *31*, 101530. [[CrossRef](#)]
33. Babu, B.; Harish, V.V.N.; Koutavarapu, R.; Shim, J.; Yoo, K. Enhanced visible-light-active photocatalytic performance using CdS nanorods decorated with colloidal SnO₂ quantum dots: Optimization of core-shell nanostructure. *J. Ind. Eng. Chem.* **2019**, *76*, 476–487. [[CrossRef](#)]
34. Thirumal, V.; Rajkumar, P.; Babu, B.; Kim, J.-H.; Yoo, K. Performance of asymmetric hybrid supercapacitor device based on antimony-titanium carbide MXene composite. *J. Alloys Compd.* **2024**, *982*, 173598. [[CrossRef](#)]
35. Babu, B.; Kim, J.; Yoo, K. Improved solar light-driven photoelectrochemical performance of cadmium sulfide-tin oxide quantum dots core-shell nanorods. *Mater. Lett.* **2020**, *274*, 128005. [[CrossRef](#)]
36. Xiao, X.; Han, B.; Chen, G.; Wang, L.; Wang, Y. Preparation and electrochemical performances of carbon sphere@ZnO core-shell nanocomposites for supercapacitor applications. *Sci. Rep.* **2017**, *7*, 40167. [[CrossRef](#)]

Disclaimer/Publisher’s Note: The statements, opinions and data contained in all publications are solely those of the individual author(s) and contributor(s) and not of MDPI and/or the editor(s). MDPI and/or the editor(s) disclaim responsibility for any injury to people or property resulting from any ideas, methods, instructions or products referred to in the content.